A nanoscale communication network scheme and energy model for a human hand scenario

Sebastian Canovas-Carrasco ✉, Antonio-Javier Garcia-Sanchez ⚲ ✉, Joan Garcia-Haro ✉

Show more ⌄

☰ Outline | ⅋ Share 🗩 Cite

Get rights and content

open access

Abstract

Real-time monitoring of medical test parameters as well as biological and chemical substances inside the human body is an aspiration which might facilitate the control of pathologies and would ensure better effectiveness in diagnostics and treatments. Future Body Area NanoNetworks (BANN) represent an ongoing effort to complement these initiatives, although due to its early stage of development, further research is required. This paper contributes with a hierarchical BANN architecture consisting of two types of nanodevices, namely, nanonodes and a nanorouter, which are conceptually designed using technologically available electronic components. A straightforward communication scheme operating at the THz band for the exchange of information among nanodevices is also proposed. Communications are conducted in a human hand scenario since, unlike other parts of the human body, the negative impact of path loss and molecular absorption noise on the propagation of electromagnetic waves in biological tissues is mitigated. However, data transmission is restricted by the tiny size of nanodevices and their extremely limited energy storing capability. To overcome this

FEEDBACK 🗩

medical parameter readings.

Keywords

Wireless nanosensor networks; Terahertz band; Energy harvesting; Nanodevice; Human-body scenario

1. Introduction

Nanonetworks will be a powerful technological solution enabling the detection, acquisition and monitoring of physical magnitudes in application scenarios which are hitherto unimaginable. It is even possible to foresee data processing, the communication of results, and decision-making tasks, all being carried out on a nanoscale level and with unprecedented accuracy. Medical parameters such as body temperature, glucose levels or cancer biomarker detection will be gathered in real-time and dispatched to remote destinations through nanodevices (in this work, for nanodevices we mean nanomachines based on electronics with a scale measured in nanometers), which will play an important role in the field of nanonetworking. In this regard, one of the most promising applications of nanonetworks is their use as Body Area NanoNetworks (BANN); in which, for instance, interconnected nanodevices flow into the bloodstream, reporting information to specialist external personnel (e.g. doctors) or information processing systems (e.g. Big Data paradigm).

However, the design, implementation and deployment of nanonetworks in a living biological environment poses considerable problems, which must be overcome; in turn presenting challenges in many different research fields such as signal propagation, antennas, and information technology, among others. The extremely high electromagnetic (EM) frequencies required for communication among nanodevices (expected in the THz band) together with the particular channel requirements in biological tissues (extremely high path loss and molecular absorption noise values) restrict signal propagation. A possible approach consi...

FEEDBACK 💬

Therefore, more effort must be devoted to developing a realistic energy model that would guarantee sufficient power to appropriately supply the nanodevices. In this paper, firstly, we contribute with the design and development of a specific energy model for a BANN, which considers and evaluates the concerns related to the channel and the nanoscale. To minimize the negative impact of signal propagation and molecular absorption losses, we consider a human hand scenario, given the thinness of its biological tissues. Unlike other BANN works, a detailed study of radio propagation losses is carried out, taking into account the most relevant biological tissues of the human hand scenario under study.

To achieve energy consumption attuned to the needs of mission-driven nanodevices, a straightforward communication scheme in a thorough design of a network architecture is proposed and assessed. Both the network architecture and communication scheme constitute the second contribution of this work, discussing the facilities for sensing a biological parameter and transmitting it outside the human body. To this end, we propose a hierarchical architecture composed of two types of nanodevices, which we also design conceptually. Namely, (i) nanonodes circulating in the bloodstream, which collect and exchange information with a (ii) nanorouter implanted into the skin of a hand. Close to the nanorouter, and outside the body, a gateway connects the BANN to the external world, via conventional technologies, such as Bluetooth or WiFi. It is worth mentioning that all the components of the nanodevices have been selected from advanced but available technologies.

Finally, our third contribution relates to energy management, in particular, to supplying the appropriate power to nanodevices to enable them to conduct their tasks. Due to the unfeasibility of manipulating them and, therefore, replacing "traditional" batteries, the power supply system in both nanonode and nanorouter, should enable energy harvesting and storage. In this endeavor, piezoelectric nanowires and a rechargeable nanocapacitor have to be integrated into the nanodevices. Considering the scenario and the architecture here proposed, the power provision for nanonodes is achieved by employing two types of energy harvesting sources: (i) the bloodstream of the human body itself, and (ii) an ultrasound external source placed in the hand. Both induce movements in the nanowires, ensuring a constant battery recharge. Conversely, the nanorouter battery is continuously recharged by the ultrasound external power supply.

The rest of the paper is organized as follows. In Section 2, we review the related work in the area. In Section 3, we propose a layered channel model that simulates the dors

FEEDBACK 💬

2. Related work

To the best of our knowledge, a realistic case of study for a BANN contributing with an exhaustive work in terms of nanodevice design, integrating communication mechanisms to extend the lifetime of nanodevices has not been reported yet in the scientific literature. In this regard, different papers have tackled specific aspects referring to nanocommunications, such as network topology, communication schemes, channel characterization, or the energy consumption of nanodevices. However, unlike our work, these nanocommunication topics are regarded as isolated islands, and a comprehensive and more practical solution which encompasses all of them is not offered.

Concerning BANN topologies, diverse studies have dealt with how a BANN should be deployed [[3], [4]], proposing a generic hierarchical architecture consisting of a nanointerface receiving external requests and returning the requested data, a nanorouter collecting data from nanonodes, and in turn, the nanonodes gathering data from the human body. However, the communication scheme portrayed did not suggest any solution to overcoming the huge absorption losses in the biological tissues at the THz band. Thus, the energy required to accomplish the communication between nanodevices must be significantly higher than the value employed in the communication schemes described in these works. As a result, the packet exchange suggested between nanorouter and nanonode cannot be feasibly implemented.

Continuing with works related to the communication scheme in a nanonetwork, in [5], a handshake-based MAC protocol for nanonetworks is proposed. In this protocol, nanodevices are able to dynamically choose different physical layer parameters based on the channel conditions and their remaining energy. Nevertheless, there are two main drawbacks not covered by this protocol. Firstly, contemplating a realistic nanonode design [6], the handshake process requires an amount of energy in the nanonode that would deplete the energy stored in its nanocapacitor without sending any useful data. Secondly, nanonodes might not have enough computational resources to find and share the optimal channel communication parameters. In [7], authors designed a routing framework for nanonetworks to optimize energy consumption, thus developing a multi-hop decision algorithm. In this approach, the nanorouter decides upon the distance to the nanonodes; if they must send the data directly to

FEEDBACK 💬

communications, considering the limited resources of nanodevices.

Regarding the THz channel characterization, in [8], a propagation model for EM communications in the THz band is developed. The radiative transfer theory and molecular absorption are considered in this work. The model accounts for the total path loss and the molecular absorption noise that a wave in the THz band experiences when propagating over very short distances. In particular, for biological tissues, the characteristics of EM waves propagating inside the human body at terahertz frequencies was studied in [1]. Based on the obtained path losses and noise level in different human tissues (skin, fat, and blood), authors evaluated the channel capacity within the human body. However, the total path loss was not computed in a realistic scenario. In this context, the work in [9], took into account the inhomogeneous structure of biological tissues to calculate path loss in a biological medium. Even though the path loss obtained was extremely accurate, a communication scheme to accomplish communication between nanodevices was not contemplated. To face these challenges, our paper considers the path loss in a human hand to properly design a communication scheme for a BANN.

With regards to energy management in a nanonetwork, the pioneering work of Jornet et al. [2], proposed a theoretical analysis of energy harvesting in a nanonetwork. This model was designed considering both the energy harvesting and the energy consumption processes. As in our paper, authors contemplated a capacitor to store energy collected from a piezoelectric nanogenerator. However, authors did not consider current technologies to estimate the maximum energy stored in a nanonode, nor higher transmitted energy values to overcome the channel loss of biological tissues in the THz band.

3. Terahertz biological channel model

In this section, the characterization of a biological channel in the THz band is proposed. The dorsum of a hand is taken as a reference scenario, which is modeled as a 4-layered structure (each layer corresponds to a specific type of biological tissue). Once the channel composition is defined, we compute the total path loss by analyzing the main electrical properties of each type of biological tissue at 1 THz. Finally, the molecular noise is also studied to determine its incidence on the communication scheme.

FEEDBACK 💬

nanorouter, the biological composition of the dorsum of the hand has been modeled as a layered structure, similar to the model proposed in previous works [[1], [9]]. The upper layer is composed of skin, split into dermis and epidermis. Both human tissues have very similar electrical properties, as demonstrated in [10], thus, in our study, we have considered both as one single tissue. The middle layer represents the subcutaneous fat, which in the back of the hand is rather thin. This thinness makes this part of the human body one of the most suitable for establishing a BANN, since the distance between the outside of the human body and the vein is fairly short (Table 1). Finally, the lower layer, which models the vein, is made up of blood. This will recreate the situation in which the nanonode is operating in the circulatory system. Both nanodevices must be encapsulated in a biocompatible capsule/artificial cell to be implanted into the human body, as cited in [11].

The thickness of each tissue, specified in Table 1, has been obtained from experimental measurements reported in scientific literature for the dorsum of the hand [[12], [13], [14], [15]]. When a range of thickness is suggested in the literature, the worst case scenario, that is, the greatest thickness, has been adopted. Finally, note that the blood layer thickness stands for the diameter of a dorsal hand vein.
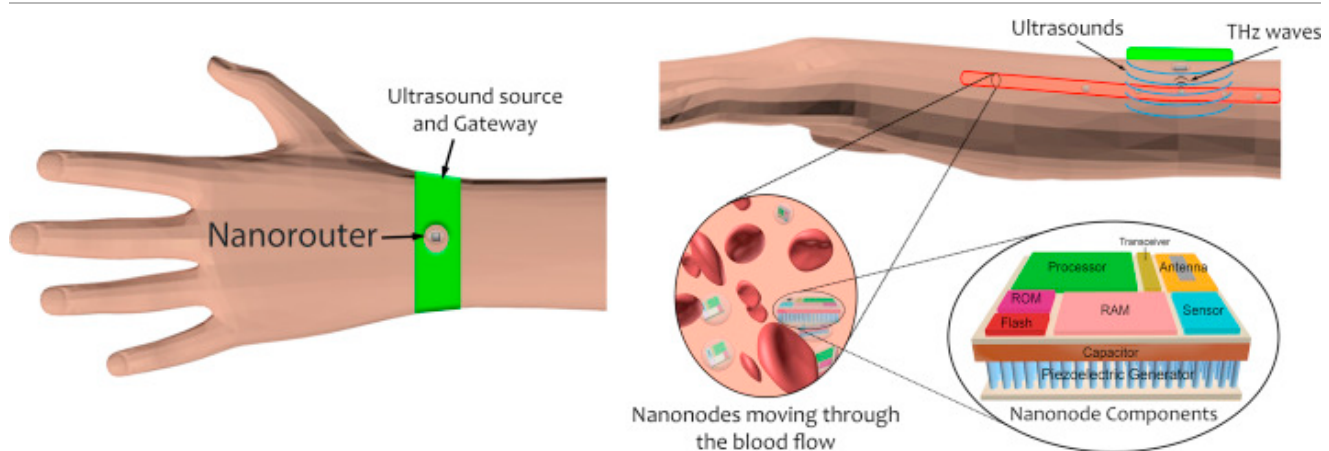
Download : Download high-res image (422KB)   Download : Download full-size image

Fig. 1. Hierarchical BANN architecture.

In our scenario, both nanorouter and nanonode are supposed to be placed ins[FEEDBACK 💬]

Table 1. Thickness of each biological tissue (dorsum of the hand).

Biological tissue	Thickness (mm)
Epidermis	0.19
Dermis	1.06
Subcutaneous fat	0.06
Blood	1.20

3.2. Path loss

The model proposed by Jornet and Akyildiz in [8] to calculate the path loss of the THz channel in water vapor paved the way for later path loss studies in biological tissues. Based on this approach, in [1], a theoretical path loss model is proposed, in which the channel losses are formulated as the addition of two contributions: the spreading loss and the molecular absorption loss. The first term represents the transmission of the EM wave in the physical medium, which can be easily modeled by the Friis path loss formula. We adapt this equation to our biological case of study, which is defined as:

$$L_{spread}(f, d) = \left(\frac{4\pi d n_m}{\lambda_0} \right)^2 \tag{1}$$

where d is the propagation distance, λ_0 is the free-space wavelength, and n_m stands for the refractive index of the medium. At a frequency of 1 THz ($\lambda_0 = 300$ μm), the spreading loss is considerably high, severely limiting the transmission range of nanonodes. This is the reason why our human body scenario sharply reduces the communication distance between the nanorouter and the nanonode.

The second term of the path loss accounts for the attenuation caused by *molecular absorption*. In general, when EM waves propagate through a material, a fraction of the EM energy radiated by a nanoantenna is converted into the internal kinetic energy of the molecules. This process depends on the working frequency and the biological tissue under considerati...

FEEDBACK 💬

where d is the propagation distance. In order to calculate the absorption path loss at 1 THz, Table 2 shows the absorption coefficient together with n_m for each tissue in the model at the required frequency [10].

Once each analytical term of the losses has been detailed, the total path loss of the channel can be expressed as follows:

$$L_{path}(f,d) = L_{spread}(f,d) * L_{abs}(f,d) = \left(\frac{4\pi d n_m}{\lambda_0}\right)^2 e^{\alpha(f)d} \tag{3}$$

Table 2. Physical properties for skin, subcutaneous fat, and blood respectively.

Biological tissue	Absorption coefficient at 1 THz (cm^{-1})	Refractive index n_m	Acoustic absorption coefficient (dB cm^{-1} MHz^{-1})	Acoustic impedance (MRayl)
Skin	**110**	**1.73**	**1.84**	**1.99**
Subcutaneous fat	80	1.50	0.6	1.38
Blood	215	1.96	0.15	1.66

Analyzing the expression (3), it can be seen that the total path loss increases as the frequency, distance or absorption of the medium (or a set of parameters) rises. To be precise in our study, the total path loss must be derived for each biological tissue, since each one will impact differently on the path loss calculation due to its specific refractive index and absorption coefficient. Therefore, to calculate $L_{path}(f,d)$ these two parameters at 1 THz and the distance of each tissue must be taken into consideration. The dependence of the total path loss for skin, fat, and blood on the distance are shown in Fig. 2, where the huge losses per length unit can be perceived. It is noteworthy that, in accordance with the work in [1], the losses caused by reflections in the interfaces between layers are not considered due to the similar electrical properties of the tissues.

FEEDBACK 💬

region, in which energy from ultrasounds can be harvested efficiently, has been considered 5 mm as a design parameter. This length is enough to ensure the straightforward integration of the ultrasound energy source into a small external wearable (e.g. a bracelet, as shown in Fig. 1). Thus, we calculate the total path loss in this range of distances, in accordance with the scheme depicted in Fig. 3.
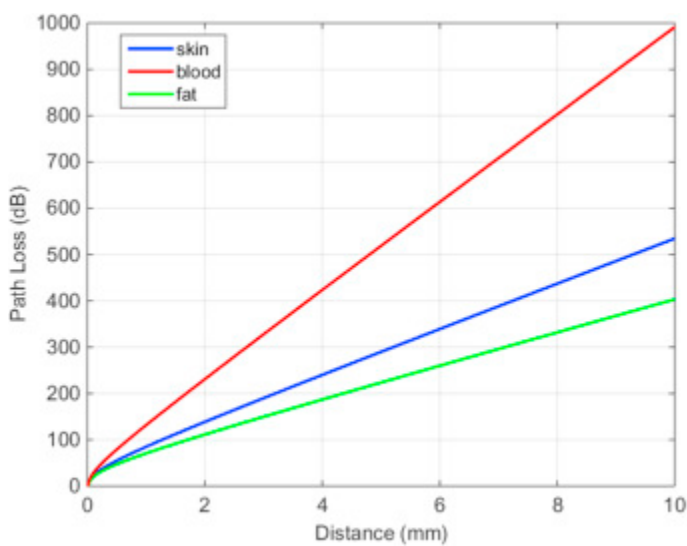
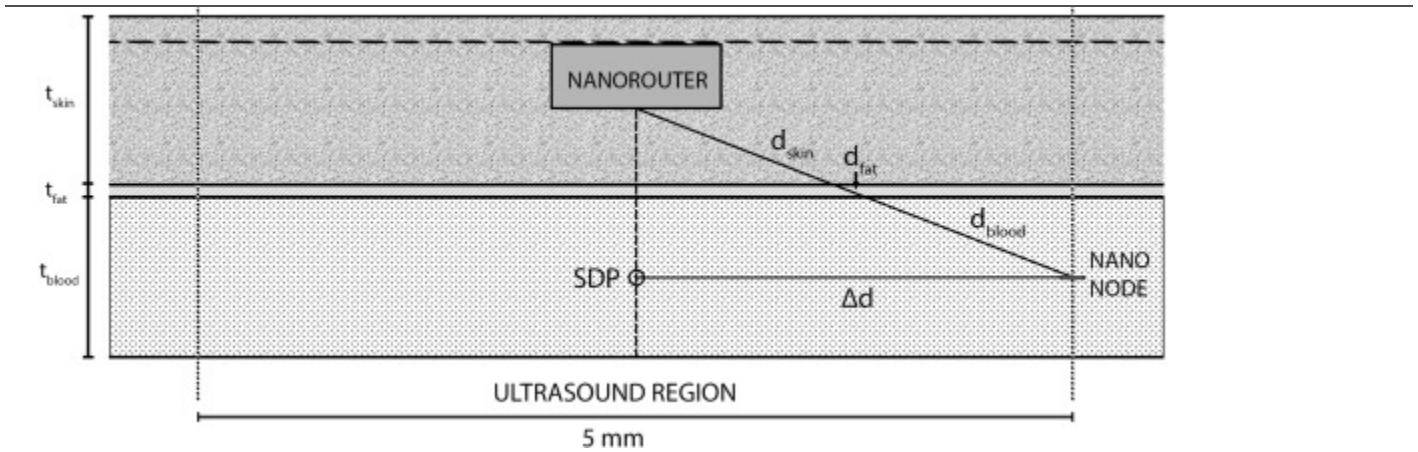Download : Download high-res image (185KB)   Download : Download full-size image

Fig. 2. Total path loss for skin, fat and blood as a function of distance at 1 THz.

Here, the distance between transmitter and receiver depends on the distance from the nanonode to the SDP (Δd). As can be seen, the fraction of distance traveled by the EM wave through the skin (d_{skin}), fat (d_{fat}), and blood (d_{blood}) also varies, which will directly affect the total path loss. Applying basic trigonometry, d_{skin}, d_{fat}, and d_{blood} as a function of Δd have been correspondingly calculated:

$$d_{skin}\left(\Delta d\right) = \sqrt{t_{skin}^2 + \left(\Delta d \frac{t_{skin}}{d_{min}}\right)^2} \tag{4}$$

$$d_{fat}\left(\Delta d\right) = \sqrt{\left(t_{skin} + t_{fat}\right)^2 + \left(\Delta d \frac{t_{skin} + t_{fat}}{d_{min}}\right)^2} - d_{skin} \tag{5}$$

FEEDBACK 💬
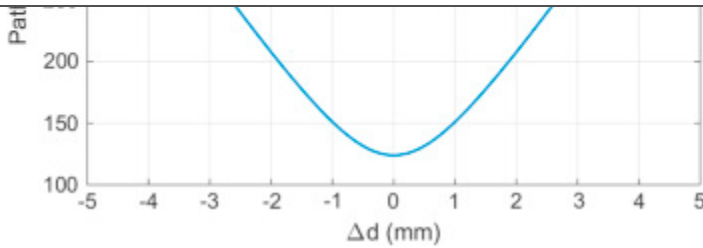
Download : Download high-res image (1MB)	Download : Download full-size image

Fig. 3. Distance scheme at the ultrasound region.

Under these conditions, substituting the specific values for n_m, $\alpha(f)$, and d for each biological tissue in the expression (3), the total path loss as the nanonode moves across the ultrasound region is shown in Fig. 4. It can be observed that the total path loss sharply decreases as the nanonode goes into the ultrasound region (getting closer to the nanorouter) and reaches its minimum value (124 dB) when Δd is equal to zero, that is, when the nanonode is in the SDP.

However, as the nanonode moves away from the SDP, the path loss quickly increases. Therefore, in order to maximize the probability of completing the communication without error (corrupted or lost information), the nanonode should be activated as close as possible to the SDP.

FEEDBACK

Fig. 4. Path loss as a function of the distance to the SDP.

3.3. Molecular absorption noise

The absorption phenomenon from molecules present in the medium, not only affects the properties of the channel in terms of attenuation, but it also introduces noise. As was studied in depth in [8], this is the major noise contribution at the THz band. The intrinsic noise caused by the electronics systems based on graphene (material proposed to build nanoantennas in most researches) can be considered negligible [[16], [17]]. To reduce the effect of molecular absorption noise, the technique proposed by Akyildiz and Jornet, based on the transmission of femtopulses, along with an On–Off Keying modulation (TS-OOK) [18], is the communication procedure chosen for the communication between nanonode and nanorouter. It employs ultra-short pulses (100 fs) to send a logical '1', while the logical '0' is transmitted as silence.

As detailed in [8], molecular noise relies on the emissivity of the channel, (ε), which can be defined as a function of the absorption coefficient $(\alpha(f))$:

$$\varepsilon\,(f,d) = 1 - e^{-\alpha(f)d} \qquad (7)$$

where d is the propagation distance. The equivalent noise temperature due to molecular absorption (T_{mol}) expressed in Kelvin is defined as:

$$T_{mol}\,(f,d) = T_0\varepsilon\,(f,d) = T_0\left(1 - e^{-\alpha(f)d}\right) \qquad (8)$$

where T_0 denotes the reference temperature, which in our case corresponds to FEEDBACK 💬

calculated by integrating $N(f,d)$ over the transmission bandwidth (B).

$$P_N(f,d) = \int_B N(f,d)df = K_B \int_B T_0 \left(1 - e^{-\alpha(f)d}\right)df \tag{10}$$

This expression computes the noise power at the receiver. However, this noise is only present when a femtopulse is propagating through the medium, that is, when a logical '1' is being transmitted. Otherwise, the noise at the receiver is nearly zero. As the time between pulses is seven orders of magnitude larger than the pulse duration, the molecular noise power should not be detected in a different pulse period, thus reducing the effect of noise in bit detection errors. As a consequence of molecular noise behavior, the noise power is added to the power transmitted, resulting in the deforming and spreading of the pulse in time (see Fig. 5). This spread is due to the relaxation time of the molecules, and it is defined as the amount of time required for excited molecules to reduce their amplitudes below 10% [19]. For this type of femtopulse, the relaxation time is between 1 and 5 ps, which is much shorter than the time between pulses (2 μs, justified in Section 4) and therefore, intersymbol interference (ISI) is unfeasible.

Hence, the molecular noise at the receiver when a logical '0' is transmitted (the transceiver remains silent), is negligible. As the electronic noise envisaged for graphene-based devices is extremely low, the difference of energy levels between the reception of a logical '1' and a logical '0' is substantial. This implies that the proposed TS-OOK modulation is robust enough to carry out the communication between nanodevices while keeping the communication process as simple and reduced in computer complexity as possible.

FEEDBACK
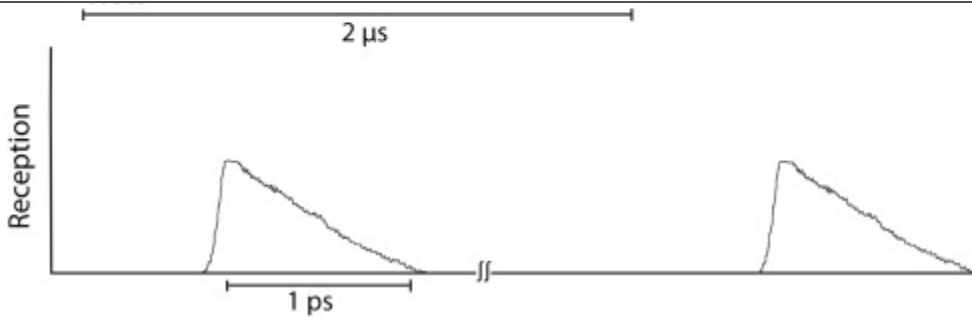
Download : Download high-res image (123KB)　　　　Download : Download full-size image

Fig. 5. Pulse spreading at the receiver due to molecular noise.

4. Nanonetworking devices: definition, features and power consumption

As previously mentioned, the limited nanodevice energy resources lead to the use of a hierarchical nanonetwork architecture to enable the junction between macro and nano worlds, following the scheme described in [20]. As shown in Fig. 1, nanonodes are the smallest nanodevices (with just a few μm in size) in our scenario and belong to the lowest level of the hierarchy, traveling through the veins. In the upper level, the nanorouter gathers the data collected by nanonodes and is able to communicate with the gateway using a THz communication system. The gateway dispatches sensor data to a traditional external system via WiFi or Bluetooth (the communication between the gateway and the nanorouter is not covered in this work). It is noteworthy that a critical aspect of properly designing the communication scheme is to determine the consumption of each nanodevice. Thus, in this section, we estimate their energy consumption based on feasible technologies in order to design a communication schedule able to work under realistic conditions.

4.1. Nanonode power consumption

The energy required by a nanonode to communicate with a nanorouter should be accurately determined to accomplish a specific application, since the operating environment conditions change according to the scenario under study (varying the amount of harvested energy). To address this problem, we refer to a previous work [6], in which the nanodevice

FEEDBACK 💬

energy nanogenerator. In order to encompass all these components in a tiny device, the dimensions of the nanonode proposed in [6] are $8 \times 8 \times 3 \, \mu$m. In the following subsections, the first four components are reviewed, paying special attention to <u>power consumption</u>, while the energy required for the nanogenerator is further analyzed in Section 5.

4.1.1. Nanoprocessor

The nanoprocessor is responsible for handling the basic protocol instructions received from the nanorouter, such as waking up/sleeping, reading data from the sensor or transmitting a frame, among others. Moreover, it will drive the operation of the remaining nanonode components to bring out the best performance of the nanodevice and ensure its proper functioning in terms of <u>sensor data collection</u>, storage, processing and communication. However, carrying out these functions is not an easy task, due to the fact that the available area in the nanonode is tightly restricted, and therefore, the resources available to the nanoprocessor will also be rather limited. This concern was extensively discussed and analyzed in [6], concluding that the SiGe-based transistor (with 7 nm technology) is the best technological option nowadays to obtain a functional nanoprocessor that satisfies the expected nanonode requirements in both size and energy consumption. Specifically, its power consumption, as analyzed, is estimated to be 140 nW for a processor working at 500 kHz. This operating frequency is enough to accomplish the aforementioned required tasks while maintaining the condition of very <u>low energy consumption</u>.

4.1.2. Memory nanomodules

Diverse types of memories are encompassed in the nanonode; each one of them intended to store information according to different purposes. Firstly, to read/write data rapidly, a RAM (Random Access Memory) module is included. Since the physical position of the data to be read or written is irrelevant, it makes RAM an appropriate solution for cache memories, where data handled by the processor will be temporarily stored. Analyzing the complete RAM family, the technological solution that best fits our particular needs is the A-RAM memory, which combines the advantages of dynamic (DRAM) and static (SRAM) memories [21]. However, due to its volatile nature, A-RAM requires a continuous refreshing signal to retain the data. Secondly, to store permanent data, such as the preset software to boot the nanodevice, a ROM module is also required. For this purpose, NOR flash memory is the best choice, since it assures low read access times, preserving an acceptable bit density and restrain

FEEDBACK 💬

EM waves, with the nanorouter of other nanonodes. The first component to deal with in our radiocommunication system is the antenna. At the nanoscale, traditional metallic antennas are not a feasible solution, since they must radiate in the range of hundreds of THz, entailing huge channel attenuation and thus, extremely short transmission coverage. Going beyond this traditional technology, research on other nanotechnological areas has led to the choice of graphene as the best material for the design and development of viable nanoantennas, able to furnish EM nanocommunications [22]. The key advantage of graphene nanoantennas is the ability to propagate surface-plasmon–polariton (SPP) waves at lower frequencies than noble metals [23]. This behavior allows graphene antennas with the size of a few μm to resonate in the range of 1 to 10 THz, which involves resonant frequencies two orders of magnitude lower than those in a nanoscale metal antenna. Moreover, a terahertz transceiver must be integrated into the nanonode in order to feed and drive the graphene nanoantenna. The terahertz transceiver proposed in [24], which was specifically designed to be integrated in a nanodevice, is composed of two blocks, an *electric signal generator* and a *graphene-based plasmonic nanotransceiver*. The former modulates an electric signal, which carries the bit stream to be sent, while the latter transforms the electric signal into an SPP wave at terahertz frequencies. Thus, the complete radiocommunication nanosystem is composed of the two blocks of the transceiver along with a graphene patch nanoantenna.

Concerning energy consumption, the proposed TS-OOK modulation is based on the use of ultra-short pulses in order to reach a high-power value using a slight amount of energy. Under this premise, the communication system is able to inject 100 pJ in a pulse of 100 fs, entailing a power transmission of 60 dBm. As was previously calculated, the total path loss at the SDP is 124 dB. Both values (power transmission and path loss) are employed to derive the received power at the receiver, which is –64 dBm. This is an acceptable value to fulfill the EM communication. The use of these femtopulses is feasible due to the very large available bandwidth (1 THz, ranging from 0.5 to 1.5 THz). Besides, in comparison with the transmission of pulses, the radiocommunication nanosystem will consume less energy in receiving a pulse from the nanorouter. So, considering the energy consumption values for a nanodevice proposed in [2], we adopt a consumption of 0.1 pJ per pulse received.

4.1.4. Nanosensor

New physical, chemical, and biological nanosensors have been developed by employing graphene and other nanomaterials in their fabrication process [[25], [26], [27], [2

application of the BANN. As each nanosensor will require a particular amount of energy to operate, we assume the generic value employed in [6], that is, 50 nW.

4.2. Nanorouter power consumption

In the same way as the nanonode, nanorouter specifications are crucial in guaranteeing appropriate performance. As the nanorouter must carry out tasks that require greater computing resources than the nanonode, its physical area should ensure the integration of an energy harvesting system large enough to power its hardware. Under these circumstances, the size envisaged for the nanorouter is $1.3 \times 1.3 \times 0.5$ mm, as will be justified in Section 5.2. Concerning the hardware included in the nanorouter, the layout will be analogous to the nanonode but on a larger scale. This increase in size, along with the increment of computing resources, involves higher energy consumption, which must be adapted to our application scenario.

On the one hand, our estimation for the power consumption of the processor is founded on the following requirements: (i) the nanorouter processor is based on the 7-nm SiGe-based transistor, and therefore, it is larger than the one included in the nanonode, coming close to the size of commercial microprocessors [29], and (ii) the operating frequency should ensure suitable performance. Therefore, as an upper limit, we consider that the nanorouter processor will consume the same energy per cycle as the processor built in [29], that is, 2.8 nW per kHz. Regarding the operating frequency, it is set to 5 MHz, since it is affordable for the energy harvesting system and should be high enough to provide the additional processing power required to manage communication with a large number of nanonodes and exchange data with the gateway. Thus, the average power consumption of the nanoprocessor including the ROM and RAM modules is 14 μW.

On the other hand, the radiocommunication system encompassed in the nanorouter would be quite similar to that of the nanonode, since the frequency range covered should be the same in both devices (in the THz band). For the sake of simplicity, in this study, we consider that the nanorouter employs the same modulation scheme as the nanonode (TS-OOK), with a pulse duration and energy which have been set to 100 fs and 100 pJ, respectively. Regarding the transmission pulse rate, we think it is reasonable that the nanorouter has to radiate at the maximum rate that a nanonode can support. According to the previously mentioned specifications for the nanonode, its nanoprocessor runs at 500 kHz, which sho

FEEDBACK

unfeasible, which leads us to look for new ways to appropriately power the nanodevice components. Nanogenerators are the most widely accepted technological solution by the scientific community [[2], [3]], and in particular, those fabricated using Zinc Oxide (ZnO) nanowires. ZnO nanowires are one of the most promising systems for energy harvesting [30], since they are able to convert mechanical strains and vibrations into electric energy due to their piezoelectric properties. To this end, nanowires are vertically arranged and firmly fixed at one end to a substrate while the other end is free, thus allowing them to bend. Under this scenario, a voltage and current are induced and collected by both electrodes (the ends of the nanowire). Once the voltage is adjusted (since the potential difference has an opposite sign depending on the nanowire movement), the energy produced is stored in a nanocapacitor to later be employed in the feeding of the nanodevice components.

In light of the network structure described in the introduction, the nanorouter will only be fed by ultrasound waves, while the nanonodes will be powered through their movement in blood flow, except for those in the acting range of ultrasounds. Thus, two different harvesting cases are studied: (i) energy harvesting from blood flow, and (ii) energy obtained from an external source through ultrasound waves.

5.1. Energy harvesting from the bloodstream

In the scenario proposed in this work, nanonodes are deployed into the blood flow of a human body to form a nanonetwork. This working environment acts on a regular basis; the strain intensity depends on the blood pressure and the frequency of the heartbeat. Under these regular conditions, the average power density produced by a ZnO nanogenerator reaches a value of 0.01 pW/μm^3 with a peak voltage of 0.7 V [31]. This value was obtained under laboratory conditions when a regular strain at a frequency of 0.3 Hz was applied. In our case, the heartbeat has a minimum frequency of 1 Hz which would triple the average power produced. However, we assume the worst case scenario since the energy harvested depends on different factors that require more exhaustive study, such as the position of the nanodevice in the vein, blood pressure or the distance to the heart. Thus, adopting the nanonode dimensions suggested in [6], the nanogenerator volume is 128 μm^3, so the envisioned average power produced by each nanonode when they are excited just by blood flow movement is 1.28 pW.

5.2. Energy harvesting from an external source

FEEDBACK 💬

operating periods are longer than those for the nanonodes.

In order to accurately estimate the power generated by ultrasounds, we follow the methodology proposed in [11] since it fits our case study. As a starting point, we set the ultrasound intensity (I_o) transmitted by the external source, which is restricted to a maximum of 720 mW/cm^2 by medical recommendations. Thus, we consider this value in order to maximize the energy harvesting. As the ultrasound signal must propagate through different biological tissues to reach nanodevices, the attenuation experienced must be taken into account. In particular, two different physical phenomena should be accounted for: (i) the absorption of energy caused by the tissues, which is converted into thermal energy, and (ii) the reflection when the tissue changes.

Similar to absorption losses in EM waves, ultrasound absorption is related with the absorption coefficient of the tissue (α) by means of the following expression:

$$\frac{I_{abs}}{I_o} = 1 - 10^{-\left(\alpha fd/10\right)} \tag{11}$$

where I_{abs} and I_o are the absorbed and transmitted ultrasound intensities, respectively, f is the ultrasound frequency in MHz, and d is the distance in cm. The ultrasound absorption coefficient values are shown in Table 2, extracted from [32].

The energy reflected at tissue interfaces is generated by the difference between their acoustic impedances. The greater the difference, the greater the amount of energy reflected. The mathematical relation between the reflected intensity (I_r) and the incident intensity (I_o) in an interface between two different materials is defined as:

$$\frac{I_r}{I_o} = \frac{(Z_2 - Z_1)^2}{(Z_2 + Z_1)^2} \tag{12}$$

where Z_1 and Z_2 are the acoustic impedances of both materials. In the case under study, there are three well-defined interfaces: air–skin, skin–fat, and fat–blood. The acoustic impedance of air is 429 Rayl (kg s^{-1} m^{-2}), while the acoustic impedance of each biological tissue is indicated in Table 2, also extracted from [32]. As can be seen, in the interface air–skin the large difference between acoustic impedances leads to an excessively high amount of energy reflected (99.91%). Therefore, the ultrasound source must touch the skin to avoid the air–skin interface and allow the ultrasound signal to directly propagate through biological tissues. In the re...

FEEDBACK 💬

$$I_{rx} = I_o 10^{-(\alpha f d/10)} \left(1 - \frac{(Z_2 - Z_1)}{(Z_2 + Z_1)^2}\right)\left(1 - \frac{(Z_3 - Z_2)}{(Z_3 + Z_2)^2}\right) \tag{13}$$

where I_o is the intensity transmitted by the external ultrasound source (720 mW/cm^2), α is the absorption coefficient in dB/(cm MHz), f is the ultrasound frequency in MHz, d is the distance in cm, Z_1, Z_2, and Z_3 are the acoustic impedances of the tissues in our model, i.e. skin, fat, and blood.

Once the ultrasound intensity at the receiver has been analytically obtained, the electric power generated by the <u>piezoelectric</u> generator per unit of area (P_{harv}) is calculated as follows:

$$P_{harv} = I_{rx}\gamma \tag{14}$$

where, γ is the piezoelectric conversion factor. According to the work in [11] and the experimental data from [33], this piezoelectric conversion factor is between 0.0055 and 0.008 with a density of 20 nanowires per μm^2. In our study, we assume the worst case to make the nanonetwork as robust as possible, that is, only the 0.55% of the mechanical energy arriving the nanogenerator is transformed into electrical energy.

At this point, the only parameter to be set is the ultrasound frequency (f). From (11), we observe that the frequency impacts on the absorption attenuation, so that higher frequencies will entail a higher absorption by the tissue. However, as the tissue thickness is rather low in the scenario under consideration, the energy absorbed is negligible for the nanorouter (less than 1% of the ultrasound energy is absorbed at an ultrasound frequency of 1 MHz), and considerably low in the case of the nanonode (0.06% of the energy lost at 10 kHz and 5.43% at 1 MHz). Consequently, the ultrasound frequency might vary within a wide range (from 10 kHz to 1 MHz) without incurring high absorption losses. Thus, we set the ultrasound frequency to 250 kHz, which is also employed in [34] to design a piezoelectric energy <u>harvester</u> for biomedical implants.

Using all the values mentioned above together with the physical parameters of the tissues specified in Table 2, the power harvested per unit of area is solved from (14) for the nanorouter (39.52 pW/μm^2), and for the nanonode (37.45 pW/μm^2).

The requirement that fundamentally affects the determination of the nanorouter size is the amount of harvested energy which, in turn, is influenced by the power consumed. In addition, another important aspect which must be taken into consideration in determin

FEEDBACK 💬

nanorouter must always remain active. Moreover, being continuously powered, communication with the gateway, which is not addressed in this work, should not affect energy consumption.

Keeping these premises in mind, the processor and memories in the nanorouter would consume 14 μW, while the radiocommunication system would transmit, at a maximum, 500 000 pulses per second (this is the value of the nanoprocessor frequency). Since the energy per pulse is 100 pJ and the time between pulses is 2 μs, the average power radiated is 50 μW. As we can observe, the total power consumed by the nanorouter is 64 μW. To feed the device continuously, the power generator must harvest this power from the external source. So, as the power harvesting harvested per unit of area is valued at 39.52 pW/μm^2, a nanorouter area of 1.66 mm^2, (e.g. a square of 1.3 $\times$ 1.3 mm) must be enough to guarantee nonstop operation. Its thickness is not limited by the generator, since the average length of ZnO nanowires is a few micrometers. Thus, we consider a conservative value of thickness of 0.5 mm.

Likewise, repeating the aim announced at the beginning of this subsection, the nanonode will harvest energy from ultrasounds when it is within the range. According to its nanogenerator area (64 μm^2), the power scavenged by the nanonode from the external source should be 2.40 nW, as calculated in [6].

6. Nanonetworking energy model and communication scheme

As mentioned before, the nanonode should accurately know when to wake up to carry out the transmission/reception tasks due to: (i) the restricted amount of energy available, and (ii) excessive path loss when it is not aligned with the nanorouter. In our transmission scheme, the recharging of the capacitors of the nanonodes relies on their movement in blood flow along with the energy harvested from ultrasound. Employing these recharge modes, nanonodes should harvest the required energy to accomplish the transmission of a complete data packet. Then, when they approach the nanorouter and enter the ultrasound region, they should wait to get as close as possible to the SDP to ensure minimum path loss and dispatch the sensor data to the nanorouter.

Under these premises, in this section we derive an energy model that makes the EM communication between nanorouter and nanonode feasible. Firstly, we determine a suitable packet size to face these energy storage restrictions. Secondly, we calculate the

FEEDBACK

proposed in [55], the total capacitance of the nanocapacitor integrated in the nanonode is 70.4 nF. Using the well-known expression, $E_{max} = \frac{1}{2}CV_g^2$, for the generator voltage (V_g) of 0.7 V, the maximum energy stored in the nanocapacitor is 17.24 nJ. As each bit is transmitted in an individual pulse and each pulse requires an amount of energy equal to 100 pJ, the maximum packet size that the nanodevice can transmit for a single active cycle is 172 bits. As can be seen, the maximum energy radiated per pulse should be around 100 pJ to ensure an acceptable packet length. Otherwise, if higher energy per pulse is used, the bit stream that the nanonode can support with a single charge would be shorter and, therefore, inadequate to design a robust communication scheme for BANN.

Therefore, taking into account the trade-off between recharge time and communication robustness, we proposed a packet size of 40 bits (5 bytes). If a higher packet size is used, the energy harvesting time would be excessively long. In this way, the first 23 bits comprise the header. This header contains the ID of each nanonode ranging from 0 to 8 388 607, so it encompasses enough IDs to identify each one of the massive number of nanonodes envisaged for a nanonetwork. This range can be divided into subranges to identify different types of nanonodes in the BANN. For instance, according to the biological magnitude to measure, IDs from 0 to 4 194 304 would correspond to temperature nanonodes, and from 4 194 304 to 8 388 607 would be reserved for glucose nanonodes. Thus, the nanonetwork can collect and process different biological samples. Furthermore, an ID must be assigned to the nanorouter. The next 16 bits are reserved for the payload, that is, the data gathered by the nanonode. In this way, each sample (analog sensor information collected by a nanosensor to later be processed and converted into digital data) can be read with a resolution of 65 536 levels, enough for the measurement of medical parameters. Finally, the last bit is a parity bit to make the communication more trustworthy and robust.

6.2. Nanonode waiting time

In order to minimize energy consumption, the nanonode remains in sleep mode whilst its nanogenerator is harvesting and storing energy from blood flow. Nevertheless, as soon as a nanonode, charged with enough energy to transmit, detects a sudden increase in the charge level (this indicates that it has entered the ultrasound region), it should wait for a fixed time span and then switch to reception mode. In this mode, the nanonode activates the transceiver to listen to the physical medium. This waiting time is set to ensure that: (i) the energy harvested from ultrasounds is equal to the energy consumption in reception mode and (ii) the

FEEDBACK 💬

energy gathered during this period is 0.168 nJ. Since the nanotransceiver consumes 0.1 pJ per pulse received and the nanorouter radiates a pulse every 2 μs, the average power consumption of the radiocommunication system will be 50 nW in reception mode. Thus, it can be activated during 3.36 ms to be exclusively fed by ultrasounds. During this short time interval, the nanorouter is able to send a maximum of 1680 bits, which is enough to send basic instructions. Hence, the nanonode stays asleep for a waiting time of 66.64 ms after the detection of ultrasounds.

6.3. Communication schedule

After defining and calculating all the parameters employed in the energy model, in this subsection we describe the transmissionschedule for our application scenario. On the one hand, the nanonodes are moving through the human body harvesting energy and recharging their nanocapacitors to store the energy required to send an entire packet. This means the charging time (t_{charge}) relies on: (i) the nanonode energy consumption, which includes the power consumption of all nanonode components, and (ii) the power harvested from the environment (P_h). Assuming the worst case scenario, (all the bits sent are 1 s) and that one bit is dispatched in each nanoprocessor clock cycle, the energy consumption to transmit a packet (E_p) is the following:

$$E_p = \frac{n_p}{f_{np}}(P_{np} + P_s) + n_p E_{pulse} \tag{15}$$

where n_p is the number of bits in a packet, f_{np} stands for the nanoprocessor operating frequency, P_{np} is the power consumed by both nanoprocessor and memories, P_s is the power consumed by the nanosensor, and E_{pulse} is the energy radiated per pulse. As the time required for the nanosensor to capture a sample depends on the type of application, we have taken as an assumption that the nanosensor will be active during the whole transmission time (t_{tx}). Therefore, since E_p should be equal to the energy harvested during t_{charge}, it can be obtained by this expression:

$$t_{charge} = \frac{E_p}{P_h} = \frac{1}{P_h}\left(\frac{n_p}{f_{np}}(P_{np} + P_s) + n_p E_{pulse}\right) \tag{16}$$

As was determined in previous sections, the value of each parameter is as follows: $P_h = 1.28$ pW, $n_p = 40$ bits, $f_{np} = 500$ kHz, $P_{np} = 140$ nW, $P_s = 50$ nW, and $E_{pulse} = 100$ pJ. Using these values, t_{charge} is approximately 52 min. A priori, this value seems too high, but bearing in mind

FEEDBACK 💬

reception mode and would take advantage of this extra energy, which would reduce the time required to recharge the nanocapacitor.

All in all, each nanonode should be flowing into the bloodstream for at least 52 min in order to accomplish the communication with the nanorouter. When the nanogenerator gathers enough energy to transmit a packet, the nanonode waits until it detects ultrasounds. Once the nanonode perceives it is within the ultrasound zone, it remains in sleep mode for 66.64 ms. Then it changes to reception mode to receive EM pulses from the nanorouter. After 3.36 ms in this state (which assures the reception of packets up to 1680 bits, allowing for a comfortable reception of control information), the nanonode transmits its entire packet (40 bits), in a transmission time t_{tx} equal to 80 μs. The communication scheme is indicated in Table 3, and the energy available in the nanodevice during the communication procedure is shown in Fig. 6. Following this procedure, the energy stored in the capacitor reaches a maximum of 4.168 nJ which guarantees the reception and transmission of information with the nanorouter in the SDP surroundings.

Table 3. Communication timing schedule.

State	Consumption (μW)	Time
Blood flow		
Sleep	~0	>52 min
Ultrasound region		
Sleep	~0	66.64 ms
Listen	0.05	3.36 ms
Transmission	50[a]	80 μs

a

50 μW is the average transmission power, calculated as: E_p / t_{tx}.
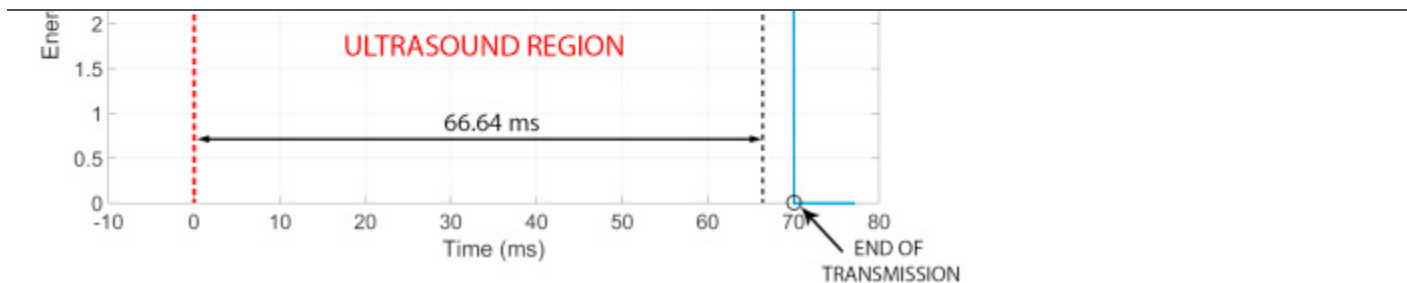
FEEDBACK

Fig. 6. Nanonode energy level during communication with the nanorouter.

7. Conclusions

In this paper, a BANN communication scheme has been realistically and accurately designed to enable the monitoring of, for instance, medical parameters between nanonodes and a nanorouter, thus overcoming the huge path loss and molecular absorption suffered in the human body. To face these limitations and show the feasibility of our BANN communication scheme, a specific human body scenario, i.e. the dorsum of the hand, has been selected. The electrical properties for its different biological tissues at 1 THz, which is the envisaged operational frequency for nanodevices have been considered. Unlike other BANN works, the adjusted thickness of the biological tissues of the hand (see Table 1) facilitates the calculation of the propagation losses. However, a huge amount of power is still required to transmit data over such short distances (a few millimeters). Therefore, the energy management required has also been analyzed and evaluated to ensure the appropriate operation of the BANN; the power consumption of each type of nanodevice proposed, as well as their energy harvesting capacity have been thoroughly derived.

Going into detail, nanonodes (in the sleeping mode) are recharged by means of: (i) the bloodstream itself, and (ii) an external ultrasound system. The nanorouter is continuously fed by the external ultrasound source system. Once the capacitor of the nanonodes has enough energy stored (4.168 nJ), the nanonodes will exchange control information and sensor acquired data with the nanorouter in the SDP surroundings. Employing this communication scheme, each nanonode is able to gather and transmit a packet (40 bits) to the nanorout

FEEDBACK 💬

Acknowledgments

Special issue articles   Recommended articles   Citing articles (41)

References

[1]   Yang K., Pellegrini A., Munoz M.O., Brizzi A., Alomainy A., Hao Y.
        Numerical analysis and characterization of THz propagation channel for body-centric nano-communications
        IEEE Trans. Terahertz Sci. Technol., 5 (2015), pp. 419-426, 10.1109/TTHZ.2015.2419823
            CrossRef   View Record in Scopus   Google Scholar

[2]   Jornet J.M., Akyildiz I.F.
        Joint energy harvesting and communication analysis for perpetual wireless nanosensor networks in the terahertz band
        IEEE Trans. Nanotechnol., 11 (2012), pp. 570-580, 10.1109/TNANO.2012.2186313
            View Record in Scopus   Google Scholar

[3]   Piro G., Boggia G., Grieco L.A.
        On the design of an energy-harvesting protocol stack for body area nano-networks
        Nano Commun. Netw., 6 (2015), pp. 74-84, 10.1016/j.nancom.2014.10.001
        Article   🅟 Download PDF   View Record in Scopus   Google Scholar

[4]   Liu B., Zhang Y., Jiang X., Wu Z.
        An energy-efficient data collection scheme in body area nanonetworks
        Proc. - 2015 3rd Int. Symp. Comput. Networking, CANDAR 2015 (2016), pp. 240-245, 10.1109/CANDAR.2015.66
            View Record in Scopus   Google Scholar

[5]   Jornet J.M., Capdevila Pujol J., Solé Pareta J.

FEEDBACK 💬

Conceptual design of a nano-networking device

Sensors, 16 (2016), p. 2104, 10.3390/s16122104

    CrossRef   View Record in Scopus   Google Scholar

[7]   Pierobon M., Jornet J.M., Akkari N., Almasri S., Akyildiz I.F.

A routing framework for energy harvesting wireless nanosensor networks in the Terahertz Band

Wirel. Netw., 20 (2014), pp. 1169-1183, 10.1007/s11276-013-0665-y

    CrossRef   View Record in Scopus   Google Scholar

[8]   Jornet J.M., Akyildiz I.F.

Channel modeling and capacity analysis for electromagnetic wireless nanonetworks in the terahertz band

IEEE Trans. Wirel. Commun., 10 (2011), pp. 3211-3221, 10.1109/TWC.2011.081011.100545

    View Record in Scopus   Google Scholar

[9]   Piro G., Bia P., Boggia G., Caratelli D., Grieco L.A., Mescia L.

Terahertz electromagnetic field propagation in human tissues: A study on communication capabilities

Nano Commun. Netw., 10 (2016), pp. 51-59, 10.1016/j.nancom.2016.07.010

    Article   Download PDF   View Record in Scopus   Google Scholar

[10]   Berry E., Fitzgerald A.J., Zinov'ev N.N., Walker G.C., Homer-Vanniasinkam S., Sudworth C.D., Miles R.E., Chamberlain J.M., Smith M.A.

Optical properties of tissue measured using terahertz-pulsed imaging

Proc. SPIE Phys. Med. Imaging (2003), p. 459, 10.1117/12.479993

    CrossRef   View Record in Scopus   Google Scholar

[11]   Donohoe M., Balasubramaniam S., Jennings B., Jornet J.M.

Powering in-body nanosensors with ultrasounds

IEEE Trans. Nanotechnol., 15 (2016), pp. 151-154, 10.1109/TNANO.2015.2509029

    CrossRef   View Record in Scopus   Google Scholar

[12]   G.C.R. Melia, M.P. Robinson, I.D. Flintoft, Development of a layered broadband model of biological materials for aerospace applications, in: EMC Eur. 2011 Yo

FEEDBACK 💬

View Record in Scopus   Google Scholar

[14]   Petrofsky J.S., Prowse M., Lohman E.
The influence of ageing and diabetes on skin and subcutaneous fat thickness in different regions of the body
J. Appl. Res., 8 (2008), pp. 55-61
View Record in Scopus   Google Scholar

[15]   Alradi A.O., Carruthers S.G.
Evaluation and application of the linear variable differential transformer technique for the assessment of human dorsal hand vein alpha-receptor activity
Clin. Pharmacol. Ther., 38 (1985), pp. 495-502, 10.1038/clpt.1985.214
CrossRef   View Record in Scopus   Google Scholar

[16]   Pal A.N., Ghosh A.
Ultralow noise field-effect transistor from multilayer graphene
Appl. Phys. Lett., 95 (2009), p. 82105, 10.1063/1.3206658
Google Scholar

[17]   Balandin A.A.
Low-frequency 1/f noise in graphene devices
Nat. Nanotechnol., 8 (2013), pp. 549-555, 10.1038/nnano.2013.144
CrossRef   View Record in Scopus   Google Scholar

[18]   Jornet J.M., Akyildiz I.F.
Femtosecond-long pulse-based modulation for Terahertz band communication in nanonetworks
IEEE Trans. Commun., 62 (2014), pp. 1742-1754, 10.1109/TCOMM.2014.033014.130403
CrossRef   View Record in Scopus   Google Scholar

[19]   Boronin P., Petrov V., Moltchanov D., Koucheryavy Y., Jornet J.M.
Capacity and throughput analysis of nanoscale machine communication through transparency windows in the terahertz band
Nano Commun. Netw., 5 (2014), pp. 72-82, 10.1016/j.nancom.2014.06.001
Article   Download PDF   View Record in Scopus   Google Scholar

FEEDBACK 💬

A-RAM: Novel capacitor-less DRAM memory

Proc. - IEEE Int. SOI Conf. (2009), pp. 4-5, 10.1109/SOI.2009.5318734

    View Record in Scopus   Google Scholar

[22]   Jornet J.M., Akyildiz I.F.

Graphene-based nano-antennas for electromagnetic nanocommunications in the terahertz band

Antennas Propag. EuCAP 2010 Proc. Fourth Eur. Conf. (2010), pp. 1-5

http://ieeexplore.ieee.org/xpls/abs_all.jsp?arnumber=5505569

    View Record in Scopus   Google Scholar

[23]   Hanson G.W.

Dyadic green's functions for an anisotropic, non-local model of biased graphene

IEEE Trans. Antennas Propag., 56 (2008), pp. 747-757, 10.1109/TAP.2008.917005

    View Record in Scopus   Google Scholar

[24]   Jornet J.M., Akyildiz I.F.

Graphene-based plasmonic nano-transceiver for terahertz band communication

8th Eur. Conf. Antennas Propag., EuCAP 2014, IEEE (2014), pp. 492-496, 10.1109/EuCAP.2014.6901799

    CrossRef   View Record in Scopus   Google Scholar

[25]   Park I., Li Z., Pisano A.P., Williams R.S.

Top-down fabricated silicon nanowire sensors for real-time chemical detection

Nanotechnology, 21 (2010), p. 15501, 10.1088/0957-4484/21/1/015501

Google Scholar

[26]   Shehada N., Brönstrup G., Funka K., Christiansen S., Leja M., Haick H.

Ultrasensitive silicon nanowire for real-world gas sensing: noninvasive diagnosis of cancer from breath volatolome

Nano Lett., 15 (2015), pp. 1288-1295, 10.1021/nl504482t

    CrossRef   View Record in Scopus   Google Scholar

[27]   Sorkin V., Zhang Y.W.

Graphene-based pressure nano-sensors

J. Mol. Model., 17 (2011), pp. 2825-2830, 10.1007/s00894-011-0972-0

FEEDBACK 💬

Nat. Nanotechnol., 9 (2014), pp. 1047-1053, 10.1038/nnano.2014.250

CrossRef   View Record in Scopus   Google Scholar

[29]   Hanson S., Seok M., Lin Y., Foo Z., Kim D., Lee Y., Liu N., Sylvester D., Blaauw D.
A low-voltage processor for sensing applications with picowatt standby mode
IEEE J. Solid-State Circuits, 44 (2009), pp. 1145-1155, 10.1109/JSSC.2009.2014205

CrossRef   View Record in Scopus   Google Scholar

[30]   Xu S., Qin Y., Xu C., Wei Y., Yang R., Wang Z.L.
Self-powered nanowire devices
Nat. Nanotechnol., 5 (2010), pp. 366-373, 10.1038/nnano.2010.46

CrossRef   View Record in Scopus   Google Scholar

[31]   Hu Y., Zhang Y., Xu C., Lin L., Snyder R.L., Wang Z.L.
Self-Powered system with wireless data transmission
Nano Lett., 11 (2011), pp. 2572-2577, 10.1021/nl201505c

CrossRef   View Record in Scopus   Google Scholar

[32]   Azhari H.
Appendix A: Typical acoustic properties of tissues
Basics Biomed. Ultrasound Eng, John Wiley & Sons, Inc, Hoboken, NJ, USA (2010),
10.1002/9780470561478.app1

Google Scholar

[33]   Wang Z.L., Song J.
Piezoelectric nanogenerators based on zinc oxide nanowire arrays
Science, 312 (2006), pp. 242-246, 10.1126/science.1124005

CrossRef   View Record in Scopus   Google Scholar

[34]   Shi Q., Wang T., Lee C.
**MEMS based broadband piezoelectric ultrasonic energy harvester (PUEH) for enabling
self-powered implantable biomedical devices**
Sci. Rep., 6 (2016), pp. 1-10, 10.1038/srep24946

View Record in Scopus   Google Scholar

[35]   El-Kady M.F., Ihns M., Li M., Hwang J.Y., Mousavi M.F., Chaney L., Lech A.T., Kaner R.B.

FEEDBACK 💬

High-resolution blood flow velocity measurements in the human finger

Magn. Reson. Med., 45 (2001), pp. 716-719, 10.1002/mrm.1096

View Record in Scopus   Google Scholar

Sebastian Canovas-Carrasco received the B.S. degree in telecommunication systems engineering and the M.S. degree in telecommunications engineering from the Universidad Politécnica de Cartagena, Spain, in 2014 and 2016, respectively, where he is currently pursuing the Ph.D. degree. His research interest includes the development of electromagnetic wireless nanonetworks and radiocommunications at the THz band.

Universidad Politecnica de Cartagena (UPCT), Spain. Since 2001, he has joined the Department of Information Technologies and Communications (DTIC), UPCT, obtaining the Ph.D. degree in 2005. Currently, he is an Associate Professor at the UPCT. He is a (co)author of more than 50 conference and journal papers, fifteen of them indexed in the Journal Citation Report (JCR). He has been the main head in several research projects in the field of communication networks and optimization, and he currently is a reviewer of several journals listed in the ISI–JCR. He is also inventor/co-inventor of 7 patents or utility models and he has been a TPC member or Chair in about thirty International Congresses or Workshops. His main research interests are in the areas of wireless sensor networks (WSNs), streaming services, Smart Grid and soil data collection.

FEEDBACK

Joan Garcia-Haro received the M.S. and Ph.D. degrees in telecommunication engineering from the Universitat Politecnica de Catalunya, Barcelona, Spain, in 1989 and 1995, respectively. He is currently a Professor with the Universidad Politecnica de Cartagena (UPCT). He is author or co-author of more than 70 journal papers mainly in the fields of switching, wireless networking and performance evaluation. Prof. Garcia-Haro served as Editor-in-Chief of the IEEE Global Communications Newsletter, included in the IEEE Communications Magazine, from April 2002 to December 2004. He has been Technical Editor of the same magazine from March 2001 to December 2011. He also received an Honorable Mention for the IEEE Communications Society Best Tutorial paper Award (1995). He has been a visiting scholar at Queen's University at Kingston, Canada (1991–1992) and at Cornell University, Ithaca, USA (2010–2011).

FEEDBACK 💬